JPn Neuroscience
The Journal of Physiology
J Physiol 593.4 (2015) pp 871–886

Chronic activation of CB2 cannabinoid receptors in the hippocampus increases excitatory synaptic transmission

Jimok Kim[1,2] and Yong Li[1]

[1] *Department of Neuroscience and Regenerative Medicine, Medical College of Georgia, Georgia Regents University, Augusta, GA 30912, USA*
[2] *Department of Neurology, Medical College of Georgia, Georgia Regents University, Augusta, GA 30912, USA*

Key points

- The effects of cannabinoids are primarily mediated by two types of cannabinoid receptors, CB1 receptors in the nervous system and CB2 receptors in the immune system.
- Recent evidence indicates that CB2 receptors are also widely expressed in the brain and involved in neuropsychiatric functions, such as schizophrenia-like behaviours, anxiety, memory, vomiting and pain.
- The cellular mechanisms by which CB2 receptors regulate neuronal functions are unknown.
- We show that chronic activation of CB2 receptors in the hippocampus for 7–10 days increases excitatory synaptic transmission, whereas short-term activation of CB2 receptors has little effect on synaptic activity.
- This study reveals a novel role of CB2 receptors in the brain, which is clearly distinct from that of CB1 receptors, and thus, will help us to understand better the diverse effects of cannabinoids in the nervous system.

Abstract The roles of CB1 cannabinoid receptors in regulating neuronal activity have been extensively characterized. Although early studies show that CB1 receptors are present in the nervous system and CB2 cannabinoid receptors are in the immune system, recent evidence indicates that CB2 receptors are also expressed in the brain. Activation or blockade of CB2 receptors *in vivo* induces neuropsychiatric effects, but the cellular mechanisms of CB2 receptor function are unclear. The aim of this study is to determine how activation of CB2 receptors present in the hippocampus regulates synaptic function. Here, we show that when organotypic cultures of rodent hippocampal slices were treated with a CB2 receptor agonist (JWH133 or GP1a) for 7–10 days, quantal glutamate release became more frequent and spine density was increased via extracellular signal-regulated kinases. Chronic intraperitoneal injection of JWH133 into mice also increased excitatory synaptic transmission. These effects were blocked by a CB2 receptor antagonist (SR144528) or absent from hippocampal slices of CB2 receptor knock-out mice. This study reveals a novel cellular function of CB2 cannabinoid receptors in the hippocampus and provides insights into how cannabinoid receptor subtypes diversify the roles of cannabinoids in the brain.

(Received 31 October 2014; accepted after revision 2 December 2014; first published online 9 December 2014)
Corresponding author J. Kim: Department of Neuroscience and Regenerative Medicine, Medical College of Georgia, Georgia Regents University, 1462 Laney Walker Boulevard, CA3004, Augusta, GA 30912, USA. Email: jimkim@gru.edu

Abbreviations ACSF, artificial cerebrospinal fluid; 2-AG, 2-arachidonoylglycerol; BSA, bovine serum albumin; CB1R, CB1 cannabinoid receptor; CB2R, CB2 cannabinoid receptor; Δ^9-THC, Δ^9-tetrahydrocannabinol; DIV, days *in vitro*; DSI, depolarization-induced suppression of inhibition; eEPSC, evoked excitatory postsynaptic current; eIPSC, evoked inhibitory postsynaptic current; ERK, extracellular signal-regulated kinase; fEPSP, field excitatory postsynaptic potential; I/O, input–output; KO, knock-out; LTP, long-term potentiation; mEPSC, miniature excitatory postsynaptic current; mIPSC, miniature inhibitory postsynaptic current; P_r, probability of release; R_m, membrane resistance; RRP, readily releasable pool; TBST, Tris-buffered saline with Tween 20.

DOI: 10.1113/jphysiol.2014.286633

Introduction

Growing interest in medical marijuana requires an accurate understanding of the effects of marijuana on the nervous system. This task is challenging because novel effects of cannabis are still being discovered. The presence of CB2 cannabinoid receptors (CB2Rs) in the brain is one such new finding, of which the functional significance has yet to be determined (Atwood & Mackie, 2010; Onaivi *et al.* 2012). Early studies showed that CB1 cannabinoid receptors (CB1Rs) are present in the nervous system and CB2Rs are in the immune system (Devane *et al.* 1988; Matsuda *et al.* 1990; Munro *et al.* 1993). Over the last decade, however, accumulating evidence has shown that CB2Rs are also widely present in the brain, in both microglia and neurons (Svíženská *et al.* 2008; Atwood & Mackie, 2010; Onaivi *et al.* 2012). Proteins and/or mRNA of the CB2R have been found in various areas of the CNS, such as the brainstem, pons, cerebellum, cerebral cortex, hippocampus, amygdala, striatum, substantia nigra, thalamus, hypothalamus and olfactory bulb (Svíženská *et al.* 2008; Atwood & Mackie, 2010). In the hippocampus, CB2R immunostaining is predominant in the soma and dendrites of pyramidal cells and some interneurons (Gong *et al.* 2006; Onaivi *et al.* 2006; Brusco *et al.* 2008), as well as in microglia (Svíženská *et al.* 2008; Atwood & Mackie, 2010). In the dendrites of hippocampal neurons, CB2Rs are located near synaptic contacts (Gong *et al.* 2006; Onaivi *et al.* 2006; Brusco *et al.* 2008).

While CB1Rs mediate most neurophysiological effects of cannabinoids, CB2Rs are also involved in neurological functions such as anxiety (García-Gutiérrez *et al.* 2012), schizophrenia-related behaviours (Ortega-Alvaro *et al.* 2011), impulsive behaviours (Navarrete *et al.* 2012), vomiting (Van Sickle *et al.* 2005) and pain (Jhaveri *et al.* 2007; Anand *et al.* 2009; Han *et al.* 2013). Evidence for the presence and function of CB2Rs in the brain is growing, but the cellular mechanisms of CB2R function are largely unknown. To understand accurately the variety of roles that cannabinoids play in the brain, it would be essential to characterize how cannabinoids act via CB2Rs.

It is important to understand the function of both CB1Rs and CB2Rs because major endocannabinoids, e.g. 2-arachidonoylglycerol (2-AG) and anandamide, and constiuents of cannabis, e.g. Δ^9-tetrahydrocannabinol (Δ^9-THC), can activate both types of receptors (Mechoulam *et al.* 1995; Showalter *et al.* 1996; Sugiura *et al.* 2000). The role of CB1Rs in the nervous system has been studied in detail (Alger, 2002; Chevaleyre *et al.* 2006; Kano *et al.* 2009; Castillo *et al.* 2012; Katona & Freund, 2012). Presynaptic CB1Rs mediate retrograde regulation of synaptic transmission in response to endocannabinoids, which originate from postsynaptic cells. Both CB1Rs and CB2Rs are coupled with $G_{i/o}$ proteins, stimulate mitogen-activated protein kinases and Akt and inhibit adenylyl cyclase (Demuth & Molleman, 2006; Fernández-Ruiz *et al.* 2007; Svíženská *et al.* 2008). The two types of receptors also have sharp contrasts. While CB1Rs are mostly expressed on presynaptic axon terminals, CB2Rs have been proposed to be postsynaptic (Gong *et al.* 2006; Onaivi *et al.* 2006; Brusco *et al.* 2008). The expression level of CB1Rs in the brain is much higher than that of CB2Rs (Onaivi *et al.* 2006). It is unknown whether such differences in receptor expression lead to functional divergence.

The proximity of neuronal CB2Rs to synapses raises the possibility that they could be involved in the regulation of synaptic function. Indeed, the spine density of hippocampal neurons in CB2R knock-out (KO) mice is lower than that of wild-type mice (García-Gutiérrez *et al.* 2013), implying that endocannabinoids contribute to the maintenance of spines via CB2Rs. It is still unclear whether and how the activation of CB2Rs regulates synaptic transmission. Furthermore, it needs to be determined whether CB2Rs in the brain are involved in synaptic modulation. We hypothesize here that the activation of CB2Rs located in the hippocampus increases spine density and excitatory synaptic transmission.

Methods

Ethical approval

All experiments were conducted in accordance with the animal use protocol that was approved by the Institutional Animal Care and Use Committee of Georgia Regents University.

Animals and hippocampal slices

Organotypic slice cultures were prepared from the hippocampus of rats and mice. Male Sprague–Dawley rats (Harlan Laboratories, Indianapolis, IN, USA) at 13–15 days of age were anaesthetized with isoflurane and decapitated. The hippocampi were dissected out and sliced at 350 μm thickness with a vibrating slicer (VT1200S, Leica, Wetzlar, Germany) in ice-cold slicing saline, which consisted of 108 mM NaCl, 2.5 mM KCl, 45 mM $NaHCO_3$, 1 mM NaH_2PO_4, 0.5 mM $CaCl_2$, 5 mM $MgSO_4$, 10 mM glucose and 0.5 mM ascorbic acid (300 mosmol kg^{-1}; bubbled with 95% O_2 and 5% CO_2). After being washed with 37°C culture medium, the slices were placed on culture membranes (EMD Millipore, Billerica, MA, USA) at the interface of the culture medium and air (with 5% CO_2) at 37°C. The medium was exchanged every 2–3 days and was composed of 50% Basal Medium Eagle (Invitrogen, Grand Island, NY, USA), 25% Earle's balanced salt solution, 25% horse serum (HyClone, Logan, UT, USA), 2 mM L-glutamine,

10 mM Hepes and an additional 5 mM glucose. Mouse slice cultures were prepared from the hippocampus of 7- to 8-day-old C57BL/6J or CB2R KO mice (Jackson Laboratory, Bar Harbor, ME, USA) of either sex with the same method as for rat cultures, except slice thickness (400 μm) and medium composition, as follows: 50% Minimum Essential Media (Invitrogen; 11090-081), 25% Hank's balanced salt solution (Invitrogen; 24020-117), 25% horse serum (HyClone), 2 mM L-glutamine, 10 mM Hepes and an additional 5 mM glucose. Slice cultures were used for experiments at 18–23 days *in vitro* (DIV). Sister slice cultures, which were made from a single animal, were divided into two groups for chronic treatment with drugs (JWH133, GP1a, SR144528 and/or PD0325901) or vehicle (0.01–0.02% ethanol). The treatment started at 11–16 DIV and lasted for 7–10 days unless otherwise noted. Slice cultures used for Figs 1*A*, *B* and *C* and 5*D* were not chronically treated.

Acute hippocampal slices were made from 41- to 46-day-old C57BL/6J or CB2R KO mice of either sex (Fig. 8). Slices were cut at 300 μm thickness in the ice-cold slicing saline, collected in a submerging chamber filled with artificial cerebrospinal fluid (ACSF), and incubated in ACSF for 30 min at 34°C and then for 1–8 h at 23°C. The ACSF contained 127 mM NaCl, 2.5 mM KCl, 26 mM $NaHCO_3$, 1 mM NaH_2PO_4, 2 mM $CaCl_2$, 2 mM $MgSO_4$ and 10 mM glucose (300 mosmol kg^{-1}) and was equilibrated with 95% O_2 and 5% CO_2. Mice used for acute slice preparation were injected once per day with JWH133 (5 mg kg^{-1}, I.P.; ~200 μl per injection) for 7–9 days starting at postnatal day 34–39. Control mice were injected with vehicle (0.9% NaCl solution with 5% DMSO and 5% Tween 80). A JWH133 stock solution for *in vivo* injection was made in DMSO at 30 mM and diluted immediately before injection in a NaCl–Tween 80 solution. CB2R KO mice (Figs 2 and 8) were bred from a pair of homozygous CB2R KO mice (Jackson Laboratory; 005786) and genotyped using REDExtract-N-Amp Tissue PCR Kit (Sigma-Aldrich, St. Louis, MO, USA) and the following primers: GGG GATCGATCCGTCCTGTAAGTCT, GACTAGAGCTTTG TAGGTAGGCGGG and GGAGTTCAACCCCATGAAGG AGTAC.

Electrophysiology

Hippocampal slices in a recording chamber were perfused with ACSF at a rate of 1.6–1.8 ml min^{-1} at 32 ± 0.5°C. All of the whole-cell voltage-clamp recordings were made from CA1 pyramidal neurons in hippocampal slice cultures at a holding potential of –70 mV. The ACSF also contained gabazine (3 μM), CGP37849 (5 μM) and tetrodotoxin (0.5 μM) for recording of miniature excitatory postsynaptic currents (mEPSCs), and 2, 3-dioxo-6-nitro-1,2,3,4-tetrahydrobenzo[f]quinoxaline-7 -sulfonamide (NBQX; 5 μM), CGP37849 (5 μM) and tetrodotoxin (0.5 μM) for recording of miniature inhibitory postsynaptic currents (mIPSCs). Evoked EPSCs (eEPSCs) were recorded in the presence of gabazine (3 μM), CGP37849 (5 μM) and NBQX (0.3 μM), and evoked IPSCs (eIPSCs) were recorded with NBQX (5 μM) and CGP37849 (5 μM) in the ACSF. Field excitatory postsynaptic potentials (fEPSPs) were recorded from the CA1 stratum radiatum of mouse acute slices without inhibitors of neurotransmitter receptors in the ACSF. The recording electrodes for fEPSPs were filled with ACSF, and their resistance was 0.5–1 MΩ.

For whole-cell recordings, the electrode resistance was 2.5–4.0 MΩ and the series resistance (<15 MΩ) was stable within 15%. The pipette solution for mEPSC recording contained 98 mM caesium methanesulfonate, 3 mM NaCl, 5 mM QX314-Cl, 4 mM $MgSO_4$, 1 mM $CaCl_2$, 10 mM EGTA, 3 mM ATP-Na, 0.3 mM GTP-Na, 30 mM Hepes and 5.4 mM biocytin (pH adjusted to 7.2 with ~20 mM CsOH, 285–287 mosmol kg^{-1}). From this pipette solution, biocytin was omitted and caesium methanesulfonate was increased to 100 mM for recording of eEPSC trains (Fig. 5*A*). A high concentration of EGTA was used in these solutions to prevent Ca^{2+}-dependent changes, if any, in EPSC amplitude. The eEPSCs and eIPSCs in Figs 1*A* and 3*B* and *C* were recorded with the pipette solution containing 110 mM caesium methanesulfonate, 10 mM NaCl, 5 mM QX314-Cl, 4 mM $MgSO_4$, 0.2 mM $CaCl_2$, 2 mM EGTA, 3 mM ATP-Na, 0.3 mM GTP-Na and 30 mM Hepes (pH adjusted to 7.2 with ~12 mM CsOH, 290–292 mosmol kg^{-1}). The concentration of EGTA was lowered to 2 mM in this solution to allow for Ca^{2+}-dependent processes. The pipette solution for mIPSCs contained 61 mM caesium methanesulfonate, 40 mM CsCl, 3 mM NaCl, 5 mM QX314-Cl, 4 mM $MgSO_4$, 1 mM $CaCl_2$, 10 mM EGTA, 3 mM ATP-Na, 0.3 mM GTP-Na and 30 mM Hepes (pH adjusted to 7.2 with ~20 mM CsOH, 285 mosmol kg^{-1}). The concentration of Cl^- was elevated to 50 mM in this solution to increase the driving force for Cl^- current.

Evoked synaptic transmission was elicited by a stimulus via a θ glass electrode (tip diameter, 10–20 μm) filled with ACSF and located in the CA1 stratum radiatum. The presynaptic stimuli were delivered every 6 s for eIPSCs, 12 s for eEPSCs (Fig. 1*A*), 20 s for fEPSPs and 60 s for a train of eEPSCs (Fig. 5*A*). The membrane resistance (R_m) was measured from steady-state current elicited by a 5 mV voltage step, every 2 min during mEPSC recordings and between individual traces during eEPSC/eIPSC recordings. Signals were amplified by a Multiclamp 700B amplifier (Molecular Devices, Sunnyvale, CA, USA), filtered at 1 (for mEPSCs) or 2 kHz and digitized at 20

(for miniature current) or 50 kHz (for evoked current and fEPSP) by a Digidata 1440 A and the Clampex 10 program (Molecular Devices).

The mEPSCs were recorded between 6 and 25 min after membrane break-in, and 300 mEPSCs per cell were used for analysis. The mEPSCs were detected based on a template waveform in the Clampfit software (Molecular Devices). The template was 30 ms long including a 6 ms baseline. For mIPSCs, 500 events per cell were used for analysis and the template was 25 ms long including a 3 ms baseline. The peak amplitudes of eEPSCs and eIPSCs were measured over a 0.4 ms window. Stimulus artifacts were graphically removed in the figures.

In the experiments of depolarization-induced suppression of inhibition (DSI; Fig. 3*C*), postsynaptic cells were depolarized to 0 mV for 5 s every 3 min, and two or three DSI trials were averaged for a given cell. The first IPSC after each depolarization was evoked 2 s after the termination of depolarization. A recovery of the eIPSC amplitudes from DSI was fitted with an exponential function, $f(t) = Ae^{-t/\tau} + C$, where t is the time of eIPSC relative to the first postdepolarization eIPSC, τ is a time constant and A and C are adjustment variables. The fitting was performed in a 90 s range that started from the first eIPSC after depolarization. The GABAergic transmission from CB1R-negative axon terminals was blocked by incubating slices with ω-agatoxin IVA (300 nM) for 15–30 min (Wilson *et al.* 2001; Fig. 3*C*).

For an analysis of eEPSC trains (60 stimuli at 20 Hz; Fig. 5*A*–*C*), 10–20 individual traces per cell were ensemble averaged. The eEPSC amplitudes in a train were normalized to the amplitude of the first eEPSC. To estimate the size of the readily releasable pool (RRP) of vesicles, the cumulative values of normalized eEPSC amplitudes were plotted against the EPSC number. Then, the data points from the 36th to 40th eEPSCs (i.e. 1.8–2.0 s after the first stimulus) were fitted with a straight line, and the y-intercept was obtained to estimate the RRP size. In the present study, the number of stimulated synapses varied randomly from experiment to experiment; therefore, RRP size was normalized to the number of stimulated synapses based on the following rationale. Given that $I = npq$ (where I is the EPSC amplitude, n is the number of stimulated synapses, p is the probability of release or P_r, and q is the quantal size) and CB2R agonists changed neither p (Fig. 5*B*) nor q (Fig. 1*C* and *D*), the normalization to the first eEPSC amplitude (I) is equivalent to the normalization to the number of stimulated synapses (n) regardless of experimental group. This process allows for comparisons of the RRP sizes across experiments.

The fEPSPs were recorded with a set of four or five presynaptic stimulus intensities. The range of stimulus intensities was determined such that input–output (I/O) relationships remained linear without saturation. The fibre volley amplitude and fEPSP slope were analysed from an ensemble average of 10–15 individual traces. The slope of fEPSP was obtained in the range of 10–60% of the peak amplitude. Stimulus artifacts were graphically removed in the figures.

The NBQX, CGP37849, gabazine and tetrodotoxin were purchased from Abcam Biochemicals (Cambridge, MA, USA); JWH133 and GP1a from R&D Systems (Minneapolis, MN, USA); SR144528 and AM251 from Cayman Chemical (Ann Arbor, MI, USA); and ω-agatoxin IVA from Peptide International (Louisville, KY, USA). Other chemicals were obtained from Sigma-Aldrich.

Confocal imaging

During mEPSC recordings, the recorded cells were filled with biocytin. After recording, the electrode was retracted slowly and the slice was washed with ACSF for 5–10 min. Then, slices were fixed in PBS with 4% formaldehyde for 5–7 days at 23°C. Slices were washed five times with PBS (10 min each) and permeabilized in PBS containing Triton X-100 (0.1%) and bovine serum albumin (BSA, 2%) for 30–60 min at 23°C. Biocytin-filled cells were stained with streptavidin–Alexa 488 (1:500) in the permeabilization solution at 23°C overnight with protection from light. Slices were then washed five times with PBS (10 min each) and mounted on glass slides with mounting medium (ProLong Gold Antifade Reagent; Invitrogen). Spines were imaged with a ×63 objective lens on a laser-scanning confocal microscope (LSM700, Zeiss, Oberkochen, Germany). Dendritic segments were selected throughout the apical dendrites but only from secondary or tertiary branches. The pixel size was 0.05 μm and the optical thickness 0.345 μm. For a given image, the maximal projection of all optical sections was used for spine analysis. The NeuronStudio software (Rodriguez *et al.* 2008) was used for automatic detection of spines and measurement of dendritic length. Spines were classified as follows. If the 'neck ratio' (head diameter/neck diameter) of a spine was >1.1, the spine was classified as a thin or mushroom spine; mushroom if the head diameter was ≥ 0.3 μm; and thin otherwise. If the neck ratio of a spine was ≤ 1.1, the spine was classified as thin or stubby; thin if the 'thin ratio' (spine length/head diameter) is > 2.5; and stubby otherwise. The minimal size of a spine was set at 10 voxels and the maximal width of a spine at 3 μm. The height of a spine was limited to 0.2–3.0 μm.

Western blot analysis

Four or five slices per condition per experiment were scraped from the culture membrane and immediately transferred to ice-cold RIPA buffer (100–125 μl; Thermo Scientific, Waltham, MA, USA), which was supplemented with a protease inhibitor cocktail (Sigma-Aldrich) and

a phosphatase inhibitor cocktail (Thermo Scientific). Then, slices were homogenized by sonication (Ultrasonic Cleaner, Branson, Danbury, CT, USA) with five 15 s pulses (one pulse every minute) at 2–5°C. The homogenates were centrifuged at 10,000*g* for 10 min at 4°C. The supernatants were collected and incubated with sample buffer (Thermo Scientific) at 70°C for 10 min to denature the proteins. Protein samples were run on a 10% polyacrylamide gel (Bio-Rad, Hercules, CA, USA) and then transferred onto polyvinylidene difluoride membranes (Thermo Scientific). After a brief wash with TBST (TBS + 0.1% Tween 20), the membranes were blocked for 1 h at 23°C in a TBST blocking solution, which contained 5% BSA, 50 mM NaF and 5 mM Na_3VO_4, and then incubated with a primary antibody overnight at 4°C. Primary antibodies (Cell Signaling Technology, Danvers, MA, USA unless otherwise noted) were diluted in the blocking solution to the following concentration: phosphorylated extracellular signal-regulated kinase (ERK) 1/2, 1:20,000; phospho-Akt, 1:50,000; pan-ERK1/2, 1:50,000; pan-Akt, 1:10,000 and β-tubulin, 1:100,000 (Thermo Scientific). The membranes were washed five times with TBST (5 min each) and incubated with HRP-conjugated anti-IgG (1:10,000 in the blocking solution; Bio-Rad) for 1 h at 23°C. Bands were visualized with a chemiluminescence detection solution (Thermo Scientific). The membranes were reused for two cycles of stripping/reprobing with different primary antibodies. Membranes were washed three times (5 min each) in stripping buffer, which contained 50 mM glycine and 0.1% SDS (pH adjusted to 2.0–2.5 with HCl), at 23°C. Western blot films were scanned on a film scanner (Epson Perfection V700) at 1200 d.p.i., and the grey scale of bands was measured with ImageJ software (NIH, Bethesda, MD, USA). The band-free background intensity was first subtracted from each band intensity, and then band intensities were normalized to the signal from sister control slices and normalized again to the β-tubulin signal from the same lane. All Western blotting experiments were duplicated with the same samples, and the duplicate values of a given sample were averaged.

Statistics

Comparisons were made only between or among sister cultures because of potential variability of data among different batches of culture. Comparisons between two groups were made using Student's *t* tests (either paired or unpaired) with a two-tailed confidence level of $P < 0.05$. Multiple comparisons were performed with one- or two-way ANOVA. Western blot data, which were normalized to control values in each experiment, were subjected to Student's paired *t* test *vs.* 100% with a two-tailed confidence level of $P < 0.05$.

Results

Chronic activation of CB2Rs increases mEPSC frequency

To test whether CB2Rs are involved in the regulation of excitatory synaptic transmission, we first examined an acute effect of a CB2R agonist on the amplitude of eEPSCs. The eEPSCs were recorded from CA1 pyramidal cells in slice cultures of the rat hippocampus, and JWH133 (200 nM), a specific CB2R agonist, was applied to the bath solution. The eEPSC amplitude was not significantly changed by the application of JWH133 for 25–30 min (94.1 ± 3.7% of baseline, $n = 6$; $P = 0.20$, Student's paired *t* test; Fig. 1*A*), indicating a lack of an acute effect of JWH133. Next, to examine the effects of longer application of JWH133 on excitatory synaptic transmission, we treated slice cultures with JWH133 (200 nM) for 3–4 days and recorded mEPSCs. By treating hippocampal slice cultures with a CB2R agonist, only the CB2Rs within the hippocampus could be activated chronically without affecting peripheral CB2Rs. The mEPSC frequency in JWH133-treated cells (1.21 ± 0.14 Hz, $n = 13$) was not significantly different from that in vehicle-treated control cells (1.20 ± 0.11 Hz, $n = 12$; $P = 0.97$, Student's unpaired *t* test; Fig. 1*B*). The mean amplitude of mEPSCs was not affected by JWH133 either (16.9 ± 0.8 pA in control cells and 17.2 ± 0.8 pA in JWH133-treated cells; $P = 0.76$, Student's unpaired *t* test; Fig. 1*B*). Then, we prolonged the duration of JWH133 treatment (200 nM) to 7–10 days. After treatment for 7–10 days, the mEPSC frequency was significantly higher in JWH133-treated cells (1.71 ± 0.16 Hz, $n = 14$) than in vehicle-treated cells (1.08 ± 0.08 Hz, $n = 14$; $P = 0.0019$, Student's unpaired *t* test; Fig. 1*C*). The mean amplitude of mEPSCs was not significantly changed by JWH133 (17.8 ± 0.5 pA in control cells and 18.4 ± 0.6 pA in JWH133-treated cells; $P = 0.44$, Student's unpaired *t* test; Fig. 1*C*). Treatment with GP1a (10 nM), another CB2R agonist, for 7–10 days also increased mEPSC frequency (1.49 ± 0.14 Hz, $n = 12$) compared with the control value (0.98 ± 0.12 Hz, $n = 12$; $P = 0.011$, Student's unpaired *t* test; Fig. 1*D*). The mEPSC amplitude was not affected by the GP1a treatment (17.7 ± 0.3 pA in control cells and 17.9 ± 0.8 pA in GP1a-treated cells; $P = 0.84$, Student's unpaired *t* test; Fig. 1*D*). The increase in mEPSC frequency appeared to be mediated specifically by CB2Rs because SR144528 (100 nM), a CB2R antagonist, prevented the effect of JWH133 on mEPSC frequency [1.15 ± 0.11 Hz ($n = 12$) in control cells and 1.16 ± 0.16 Hz ($n = 10$) in cells treated with both SR144528 and JWH133 for 7–10 days; $P = 0.99$, Student's unpaired *t* test; Fig. 1*E*]. Chronic treatment with SR144528 alone for 7–10 days had no effect on mEPSC frequency ($P = 0.85$, Student's unpaired *t* test) or amplitude ($P = 0.32$, Student's unpaired *t* test; $n = 10$ in each group; Fig. 1*F*). These results suggest that

chronic (7–10 days) activation of CB2Rs present in the hippocampus increases mEPSC frequency, while acute activation CB2Rs has little effect on excitatory synaptic transmission.

We further tested the specificity of JWH133 on CB2R using CB2R KO mice. First, we confirmed that JWH133 treatment could also increase mEPSC frequency in hippocampal slice cultures made from C57BL/6J mice, which are the congenic control for CB2R KO mice. In slice cultures from C57BL/6J mice, mEPSCs in cells treated with JWH133 (200 nM, 7–8 days) were more frequent (1.42 ± 0.17 Hz, $n = 17$) than those in vehicle-treated cells (0.91 ± 0.05 Hz, $n = 16$; $P = 0.009$, Student's unpaired t test; Fig. 2*A*). The mEPSC amplitude (18.3 ± 0.8 pA) was not affected by the treatment compared with the control value (18.0 ± 0.5 pA). In contrast, treatment of slice cultures made from CB2R KO mice with JWH133 (200 nM, 7–8 days) did not affect mEPSCs. The mEPSC frequency in CB2R KO slices (1.15 ± 0.09 Hz, $n = 14$) was similar to that in vehicle-treated slices (1.16 ± 0.09 Hz, $n = 14$; $P = 0.99$, Student's unpaired t test; Fig. 2*B*). The mEPSC amplitude was not affected by JWH133 either (17.3 ± 0.7 pA in vehicle-treated cells and 18.3 ± 0.5 pA in JWH133-treated cells; $P = 0.26$, Student's unpaired t test; Fig. 2*B*). Given that a JWH133-mediated increase in mEPSC frequency was blocked by a CB2R antagonist (Fig. 1*E*) and absent from CB2R KO tissues (Fig. 2*B*), the effect of the CB2R agonist on mEPSC frequency is likely to be mediated specifically by CB2Rs.

Activation of CB2Rs has little effect on GABAergic synapses

To test the effects of a CB2R agonist on GABAergic transmission, we recorded mIPSCs from CA1 pyramidal cells after treating slice cultures of the rat hippocampus with JWH133 (200 nM) or vehicle for 7–10 days. The mean frequencies of mIPSCs were 7.61 ± 0.45 Hz ($n = 16$) in control cells and 7.78 ± 0.41 Hz ($n = 16$) in JWH133-treated cells ($P = 0.79$, Student's unpaired t test; Fig. 3*A*). The mean amplitudes were 32.3 ± 1.2 pA in control cells and 30.6 ± 0.7 pA in JWH133-treated cells ($P = 0.21$, Student's unpaired t test; Fig. 3*A*). Therefore, the effect of chronic activation of CB2Rs is specific for glutamatergic, not GABAergic, synapses. We also tested

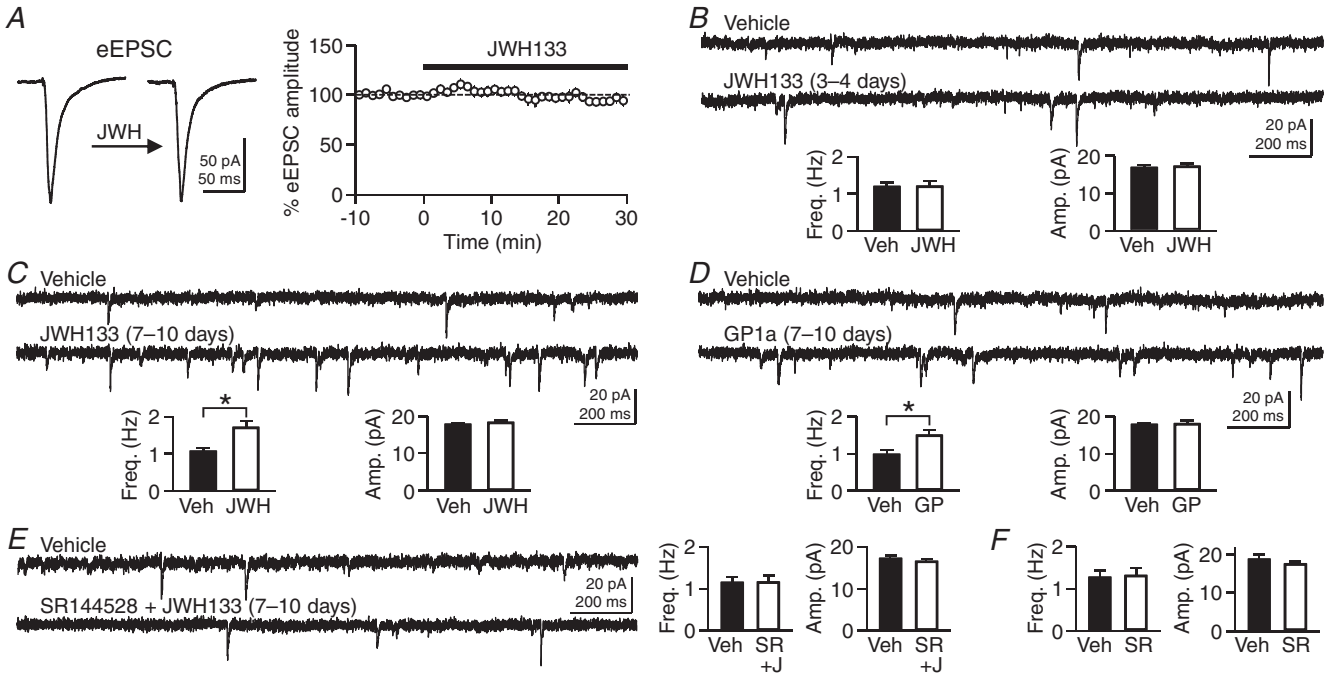

Figure 1. Chronic activation of CB2 cannabinoid receptors (CB2Rs) increases the frequency of miniature excitatory postsynaptic current (mEPSC)
A, evoked excitatory postsynaptic currents (eEPSCs) were recorded from CA1 pyramidal neurons in rat hippocampal slice cultures, and JWH133 (200 nM), a CB2R agonist, was applied to the bath solution. *B*, rat hippocampal slice cultures were treated with JWH133 (200 nM) for 3–4 days. Miniature EPSCs were recorded from CA1 pyramidal neurons in the absence of JWH133 in the bath solution. *C*, after treatment of slice cultures with JWH133 (200 nM) for 7–10 days, mEPSCs were recorded from CA1 pyramidal neurons. $^*P = 0.0019$, Student's unpaired t test. *D*, mEPSCs in cells treated with GP1a (10 nM), another CB2R agonist, for 7–10 days were more frequent than those in control cells. $^*P = 0.011$, Student's unpaired t test. *E*, treatment of slice cultures with both SR144528 (100 nM), a CB2R antagonist, and JWH133 (200 nM) for 7–10 days had no effect on mEPSCs. *F*, treatment with SR144528 (100 nM) alone did not alter mEPSCs. Error bars indicate SEM.

whether JWH133 has an acute effect on inhibitory synaptic transmission. Bath application of JWH133 (200 nM) for 25–30 min did not significantly change the mean amplitude of eIPSC (103 ± 6% of baseline, $n = 6$; $P = 0.78$, Student's paired t test; Fig. 3*B*), implying a lack of an acute effect on GABAergic transmission.

Although the CB2R drugs used in this study are specific for CB2Rs, they can also bind to CB1Rs at high concentrations. We tested whether JWH133 activates or SR144528 blocks CB1Rs. Given that CB1Rs are highly expressed in GABAergic axon terminals in the hippocampus (Katona *et al.* 1999; Marsicano & Lutz, 1999), activation of CB1Rs should suppress eIPSC amplitudes. However, JWH133 did not reduce eIPSCs even though the eIPSCs were susceptible to CB1R-medaited reduction as assayed by the presence of DSI (Fig. 3*B*). This result suggests that the CB2R agonist did not effectively activate CB1Rs. In addition, SR144528 (200 nM) did not block DSI, a CB1R-mediated process, when bath applied for 10–20 min ($n = 5$; Fig. 3*C*), indicating that the CB2R antagonist did not inhibit CB1Rs. Neither the amplitude of the first eIPSC after depolarization nor the time course of eIPSC recovery from DSI was affected by SR144528 ($P > 0.05$, Student's paired t tests; Fig. 3*C*). As a control, AM251 (300 nM; a specific CB1R antagonist) completely blocked DSI when bath applied for 7–11 min ($n = 5$; Fig. 3*C*). Given that the experiment in Fig. 3*C* was focused on DSI, DSI was maximized by incubating slices for 15–30 min with ω-agatoxin IVA (300 nM), which blocks the GABA release from CB1R-negative axon terminals (Wilson *et al.* 2001). These data suggest that JWH133 and SR144528 at the concentrations we used in our experiments had little off-target effect on CB1Rs.

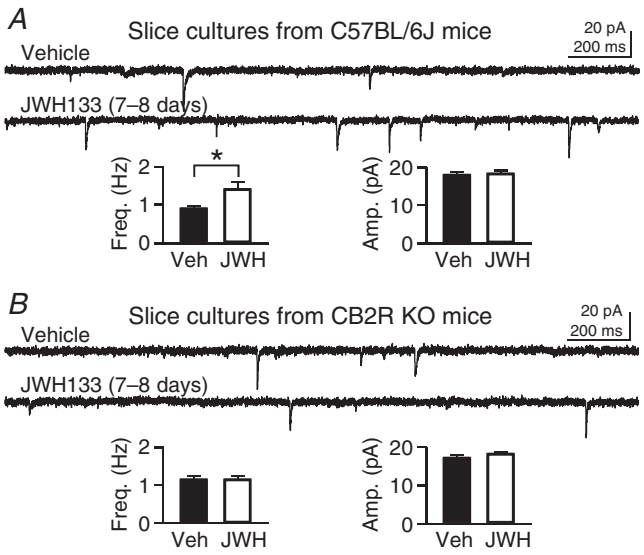

Figure 2. JWH133-induced increase in mEPSC frequency is absent from slice cultures made from CB2R knock-out (KO) mice
A, hippocampal slice cultures made from C57BL/6J mice were treated with JWH133 (200 nM) for 7–8 days. Miniature EPSCs were recorded from CA1 pyramidal neurons. $^*P = 0.009$, Student's unpaired t test. *B*, slice cultures were made from the hippocampus of CB2R KO mice. Treatment with JWH133 (200 nM) for 7–8 days had no effect on mEPSCs in CA1 pyramidal cells. Error bars indicate SEM.

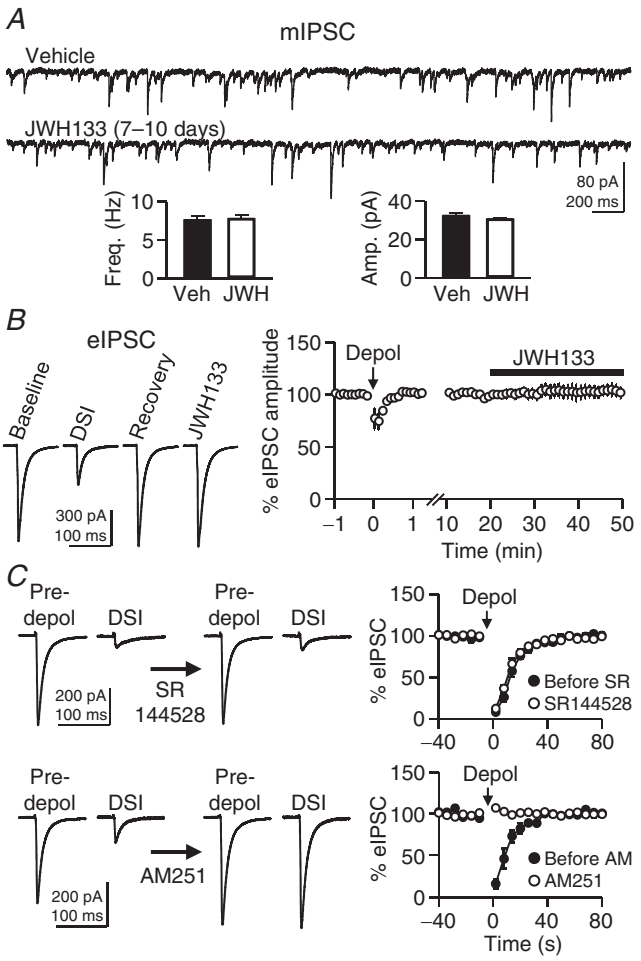

Figure 3. The effects of JWH133 on GABAergic transmission and tests for the specificity of CB2R drugs
A, rat hippocampal slice cultures were treated with JWH133 (200 nM) for 7–10 days, and miniature inhibitory postsynaptic currents (mIPSCs) were recorded from CA1 pyramidal neurons. *B*, evoked inhibitory postsynaptic currents (eIPSCs) were recorded from CA1 pyramidal neurons in rat hippocampal slice cultures, and JWH133 (200 nM), a CB2R agonist, was applied to the bath solution. Before the JWH133 application, postsynaptic cells were depolarized to 0 mV for 5 s to induce DSI, which is CB1R-mediated suppression of IPSCs. The eIPSC trace for DSI is an average of the first two eIPSCs after depolarization. *C*, DSI elicited by postsynaptic depolarization to 0 mV for 5 s was measured before and during bath application of SR144528 (200 nM; 10–20 min) or AM251 (300 nM; 7–11 min). Two eIPSCs after depolarization were averaged for the DSI traces. Error bars indicate SEM.

Chronic activation of CB2Rs increases dendritic spine density

To investigate cellular mechanisms of the CB2R-induced increase in mEPSC frequency, we hypothesized that spine density might be increased by chronic activation of CB2Rs. After 7–10 days of treatment, the mean spine density of JWH133- or GP1a-treated cells ($1.26 \pm 0.12\ \mu m^{-1}$, $n = 12$) was significantly higher than that of control cells ($1.03 \pm 0.12\ \mu m^{-1}$, $n = 11$; $P = 0.0018$, Student's unpaired t test; Fig. 4*A*). Given that the JWH133- and GP1a-treated groups ($n = 6$ each) had similar values of spine density ($P = 0.30$, Student's unpaired t test), we pooled the data from the two groups. The CB2Rs specifically mediated the increase in spine density because SR144528 blocked this effect of JWH133 [$1.01 \pm 0.10\ \mu m^{-1}$ ($n = 6$) in control cells and $1.04 \pm 0.15\ \mu m^{-1}$ ($n = 6$) in cells treated with both SR144528 and JWH133; $P = 0.66$, Student's unpaired t test; Fig. 4*A*]. The spine types were segregated based on morphology into stubby, thin and mushroom spines, and the CB2R-induced increase in density was limited to thin spines (Fig. 4*B* and *C*).

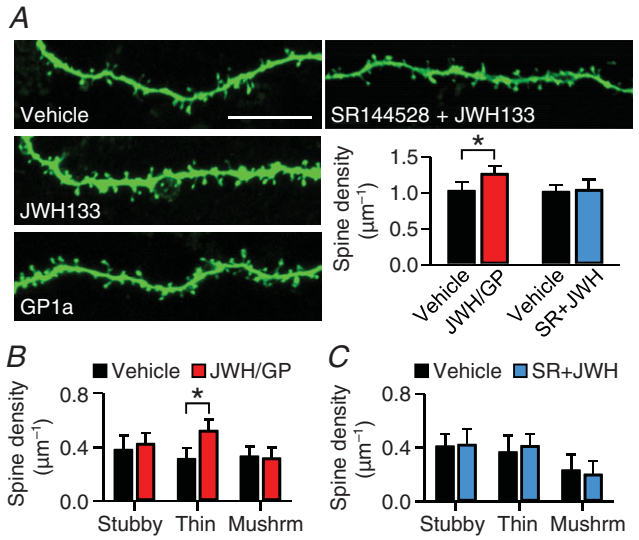

Figure 4. Chronic activation of CB2Rs for 7–10 days increases the density of dendritic spines
A, confocal micrographs show the dendrites of biocytin-filled CA1 pyramidal neurons in rat hippocampal slice cultures treated with vehicle, JWH133 (200 nM), GP1a (10 nM) or both SR144528 (100 nM) and JWH133. The bar graphs summarize the quantification of spine densities. Data from JWH133- and GP1a-treated cells were pooled. $^*P = 0.0018$, Student's unpaired t test. Scale bar, 10 μm. *B*, spines analysed in *A* were divided into stubby-, thin- and mushroom-type spines based on morphology. $^*P = 0.000026$, Student's unpaired t test. *C*, analysis of spine subtypes in slices treated with both SR144528 and JWH133. Error bars indicate SEM.

Activation of CB2Rs has little effect on presynaptic release properties and postsynaptic chloride conductance

We examined whether presynaptic properties, such as P_r and the size of RRP, also contributed to the increase in mEPSC frequency. From a train of eEPSCs (20 Hz for 3 s; Fig. 5*A*), the facilitation of the first five EPSCs was used to compare P_r among vehicle-, JWH133- and GP1a-treated synapses. Short-term facilitation was not significantly different among the three groups ($P = 0.29$, two-way ANOVA; Fig. 5*B*). The second eEPSC amplitudes (i.e.

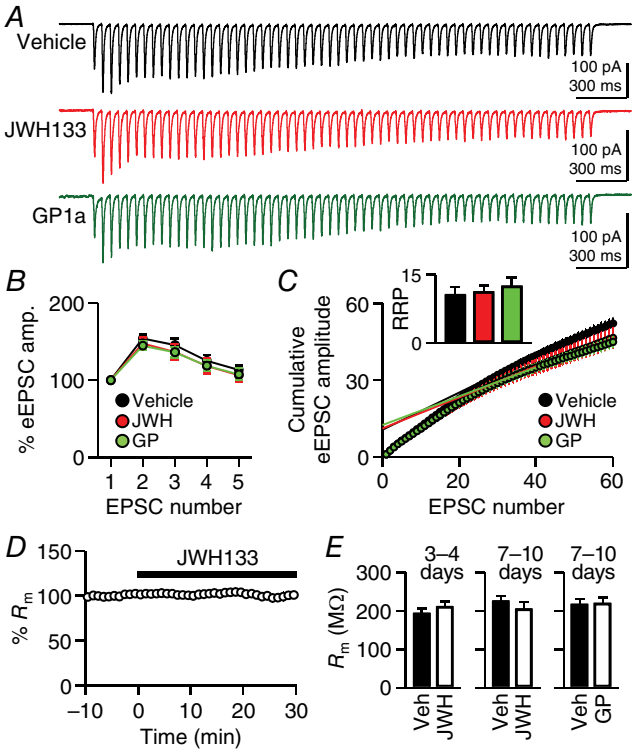

Figure 5. Activation of CB2Rs does not affect presynaptic release properties or the resting chloride conductance
A, rat hippocampal slice cultures were treated with vehicle, JWH133 (200 nM) or GP1a (10 nM) for 7–10 days. Trains of eEPSCs (20 Hz for 3 s) were recorded from CA1 pyramidal cells. An ensemble average was made from 10–20 traces. *B*, short-term facilitation of the first five eEPSC amplitudes in the 20 Hz train shown in *A*. The eEPSC amplitudes were normalized to the first eEPSC amplitude of the train. *C*, from the 20 Hz trains, cumulative amplitudes of eEPSCs, after being normalized to the first eEPSC, were plotted against the eEPSC number. For each cell, the data points from the 36th–40th EPSCs were extrapolated to the y-axis. Inset, the mean sizes of the readily releasable pool (RRP), in multiples of the first eEPSC amplitude. *D*, membrane resistance (R_m) was measured from CA1 pyramidal cells, and JWH133 was applied to the bath solution. The data were analysed and pooled from the cells in Figs 1*A* and 3*B*. *E*, R_m was measured from cells treated with JWH133 or GP1a. The treatment duration is shown above each graph. The data are from the cells in Fig. 1*B*–*D*. Error bars indicate SEM.

paired-pulse ratios) were 154 ± 6, 148 ± 8 and 145 ± 5% of the first one in vehicle-, JWH133- and GP1a-treated cells, respectively ($n = 8$ per group). This result suggests that P_r was not significantly altered by chronic activation of CB2Rs for 7–10 days.

The RRP size was estimated from cumulative amplitudes of eEPSCs in a 20 Hz train (Schneggenburger *et al.* 1999; Fig. 5*C*). When the 36th–40th eEPSCs were used for the extrapolating method of estimation, the RRP sizes, which were normalized to the first eEPSC amplitude, were similar among the three groups, at 10.6 ± 1.7, 11.2 ± 1.4 and 12.5 ± 1.8 times the first EPSC amplitude for control, JWH133 and GP1a groups, respectively ($n = 8$ per group; $P = 0.71$, ANOVA; Fig. 5*C*). This method for the estimation of RRP sizes is based on the kinetics of RRP depletion and/or refilling in autaptic culture synapses (Rosenmund & Stevens, 1996; Stevens & Williams, 2007). As the kinetics of RRP dynamics in organotypic culture synapses are uncertain, we also analysed eEPSCs at other time points and again found no differences. For control, JWH133 and GP1a groups, respectively, the RRP sizes estimated from the 26th–30th eEPSCs were 6.1 ± 1.3, 6.5 ± 0.7 and 7.6 ± 1.3 ($P = 0.62$, ANOVA); and the estimates from the 41st–50th eEPSCs were 14.0 ± 2.0, 12.7 ± 1.3 and 15.0 ± 2.1 ($P = 0.69$, ANOVA). Together, presynaptic properties such as P_r and RRP sizes were unaffected by chronic treatment with CB2R agonists, and thus are unlikely to be related to the changes in mEPSC frequency.

In the neocortex of 14- to 19-day-old rats, bath-applied JWH133 decreases R_m of pyramidal neurons by opening Cl^- channels (den Boon *et al.* 2012). Reduction in the intrinsic excitability of neurons may result in an increase in mEPSC frequency via homeostatic plasticity (Burrone *et al.* 2002). Although our pipette solutions prevented the detection of K^+-mediated changes in R_m because of Cs^+ and QX314, they allowed for the measurement of any changes in Cl^- conductance. In our experiment, however, bath-applied JWH133 (200 nM) did not change R_m of CA1 pyramidal neurons in slice cultures of the rat hippocampus (99.1 ± 3.9%; $n = 12$; $P = 0.86$, Student's paired t test; Fig. 5*D*). The R_m of JWH133-treated cells (200 nM for 3–4 days; 211 ± 13 MΩ, $n = 13$) was not significantly different from that of vehicle-treated cells (193 ± 13 MΩ, $n = 12$; $P = 0.33$, Student's unpaired t test; Fig. 5*E*). The R_m was not affected by 7–10 days of treatment with 200 nM JWH133 ($n = 14$; $P = 0.38$, Student's unpaired t test) or 10 nM GP1a ($n = 12$; $P = 0.89$, Student's unpaired t test) compared with vehicle-treated cells (Fig. 5*E*). This result is not consistent with changes in Cl^- conductance by a CB2R agonist applied either acutely or chronically. It remains to be determined whether CB2Rs modulate the excitability of hippocampal neurons by altering K^+ conductance.

Long-term activation of CB2Rs phosphorylates ERK1/2

The CB2R is coupled with $G_{i/o}$ protein to stimulate ERK and/or Akt (Demuth & Molleman, 2006; Fernández-Ruiz *et al.* 2007; Svíženská *et al.* 2008). We tested which kinase was activated, i.e. phosphorylated, by chronic treatment with a CB2R agonist. After a 7–10 day treatment with vehicle, JWH133 or GP1a, the protein levels of phosphorylated ERK1/2 and pan-ERK1/2 were analysed with the Western blotting method. The levels of phospho-ERK1/2 in JWH133- and GP1a-treated slices were 132 ± 9 ($P = 0.011$, Student's paired t test *vs.* 100%) and 156 ± 16% ($P = 0.011$) of the control value, respectively ($n = 8$ experiments; Fig. 6*A*). However, the level of pan-ERK1/2 was affected by neither JWH133 (99 ± 5%; $P = 0.86$) nor GP1a (90 ± 5%; $P = 0.066$; Fig. 6*A*). As a result, the ratio of phospho- to pan-ERK1/2 was significantly increased by either JWH133 (138 ± 14%; $P = 0.032$) or GP1a (180 ± 22%; $P = 0.0078$). In contrast, the levels of phospho-Akt and pan-Akt in JWH133- or GP1a-treated slices were not significantly different from those of control slices ($P > 0.1$; Fig. 6*B*). The ratio of phospho- to pan-Akt was 98 ± 6% ($P = 0.74$, Student's paired t test *vs.* 100%) in JWH133-treated slices and 105 ± 6% ($P = 0.41$) in GP1a-treated slices ($n = 8$ experiments; Fig. 6*B*). This result shows that, in our treatment conditions, CB2R agonists stimulated phosphorylation of ERK1/2 but not Akt.

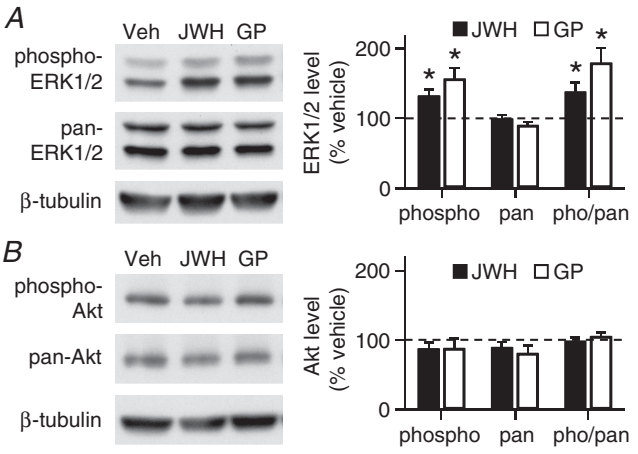

Figure 6. Chronic activation of CB2Rs increases the phosphorylation of extracellular signal-regulated kinase (ERK) 1/2
A, Western blot analysis of phosphorylated ERK1/2 and pan-ERK1/2 in rat hippocampal slice cultures treated with JWH133 (200 nM) or GP1a (10 nM) for 7–10 days. The data of phospho-ERK1/2 and pan-ERK1/2 are shown as a percentage of the control values in sister cultures. In each experiment, data were normalized to β-tubulin values. *$P < 0.05$, Student's paired t test *vs.* 100%. *B*, the levels of phosphorylated Akt or pan-Akt were not affected by treatment with JWH133 or GP1a. Error bars indicate SEM.

Phosphorylation of ERK contributes to the CB2R-medited increases in mEPSC frequency and spine density

To test whether phosphorylation of ERK contributed to the CB2R-induced increases in mEPSC frequency and spine density, we blocked ERK phosphorylation with PD0325901 (100 nM), an inhibitor of MEK1 and MEK2, both of which phosphorylate ERK. Treatment of slice cultures with PD0325901 alone (100 nM) for 7–10 days preserved glutamatergic synapses, because mEPSC frequency (1.01 ± 0.10 Hz, $n = 11$) was unaffected compared with the control value (1.16 ± 0.09 Hz, $n = 11$; Fig. 7*A*). When co-treated with PD0325901, JWH133 did not increase mEPSC frequency (0.98 ± 0.10 Hz, $n = 11$; $P = 0.38$, ANOVA for the three groups; Fig. 7*A*). The mEPSC amplitudes of the three groups were not significantly different from each other (17.0 ± 0.5 pA in control cells, 16.5 ± 0.6 pA in PD0325901-treated cells and 15.7 ± 1.1 pA in PD0325901/JWH133-treated cells; $P = 0.50$, ANOVA; Fig. 7*A*). This result supports the idea that ERK phosphorylation might be involved in the JWH133-induced increase in mEPSC frequency. The effect of PD0325901 on spine density was also tested. The mean spine density in cells treated with PD0325901 alone (1.07 ± 0.18 μm^{-1}, $n = 7$) or with PD0325901 and JWH133 (1.04 ± 0.12 μm^{-1}, $n = 8$) was not significantly different from the spine density of vehicle-treated cells (1.06 ± 0.13 μm^{-1}, $n = 11$; $P = 0.93$, ANOVA; Fig. 7*B*). There was no difference among the three groups in the densities of stubby ($P = 0.69$, ANOVA), thin ($P = 0.41$) or mushroom spines ($P = 0.49$; data not shown).

We examined whether PD0325901 indeed blocked the JWH133-induced increase in ERK phosphorylation. Treatment with PD0325901 alone for 7–10 days reduced the level of phosphorylated ERK1/2 compared with vehicle treatment (17 ± 2%, $n = 5$; $P < 0.0001$, Student's paired t test *vs.* 100%; Fig. 7*C*), suggesting that PD0325901 blocked the basal phosphorylation of ERK1/2. The mean level of phospho-ERK1/2 in slice cultures treated with PD0325901 and JWH133 (19 ± 5%) was similar to that of PD0325901-treated slices ($P = 0.75$, Student's paired t test; Fig. 7*C*), indicating that PD0325901 also blocked a JWH133-induced increase in ERK phosphorylation. Levels of pan-ERK1/2 were increased by a similar amount (~30%) in both PD0325901-treated and PD0325901/JWH133-treated slices ($P = 0.38$, Student's paired t test; Fig. 7*C*). As a result, the ratio of phospho- to pan-ERK1/2 levels in PD0325901/JWH133-treated slices was not significantly different from that of PD0325901-treated slices ($P = 0.69$, Student's paired t test; Fig. 7*C*). Interestingly, in slices treated with PD0325901 alone, a reduction in the basal phosphorylation of ERK1/2 did not induce a significant decrease in mEPSC frequency or spine density (Fig. 7*A* and *B*), implying that the ERK-mediated regulation of mEPSCs and spines may not be bidirectional.

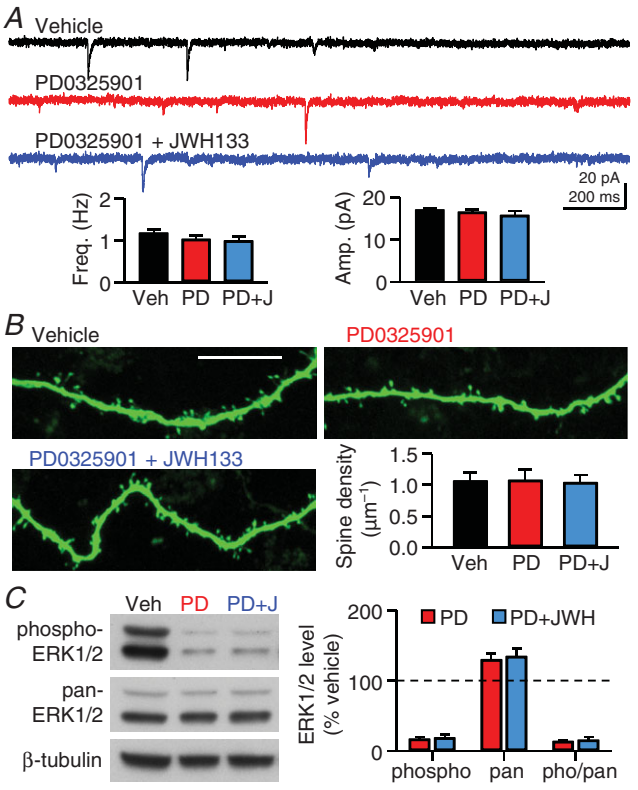

Figure 7. Phosphorylation of ERK is involved in the CB2R-induced increases in mEPSC frequency and spine density
A, mEPSCs were recorded from CA1 pyramidal cells in rat hippocampal slice cultures treated with PD0325901 (100 nM) alone or with both PD0325901 and JWH133 (200 nM) for 7–10 days. *B*, confocal micrographs of biocytin-filled dendrites of CA1 pyramidal neurons. Rat hippocampal slice cultures were treated with the indicated drugs for 7–10 days. Scale bar represents 10 μm. *C*, Western blot analysis of phosphorylated ERK1/2 and pan-ERK1/2 in rat hippocampal slice cultures treated with PD0325901 or with both PD0325901 and JWH133 for 7–10 days. Error bars indicate SEM.

Administration of a CB2R agonist *in vivo* increases excitatory synaptic transmission

Use of hippocampal slice cultures is essential for activation of CB2Rs only within the hippocampus. However, it is uncertain whether a CB2R agonist *in vivo* can also enhance excitatory synaptic transmission when administered in intact animals. We used mice for this experiment to use a CB2R KO strain. C57BL/6J mice (P34–39) were injected with JWH133 (5 mg kg^{-1}, I.P.) once per day for 7–9 days. The efficacy of excitatory synaptic transmission was assayed by constructing I/O curves of fEPSPs recorded from the CA1 area of acute hippocampal slices

made from treated mice 24 h after the last injection. The presynaptic activity of afferent input was measured as the amplitude of the presynaptic fibre volley, and the postsynaptic response was assessed by the rising slope of fEPSP. The I/O relationship was steeper in JWH133-injected C57BL/6J mice (n = 11 slices from five mice) than in vehicle-injected mice (n = 12 slices from four mice; P = 0.0009, Student's unpaired t test on the slope of the I/O curves; Fig. 8*A* and *B*), implying that the synaptic response per action potential was increased. However, in CB2R KO mice, administration of JWH133 for 7–9 days had no effect on the I/O relationship (n = 16 from three mice) compared with the vehicle effect in CB2R KO mice (n = 13 from three mice; P = 0.67, Student's unpaired t test; Fig. 8*C* and *D*). This result suggests that chronic activation of CB2Rs in intact mice also increased excitatory synaptic transmission. Our study, however, leaves it to be determined whether CB2R KO *per se* affects synaptic transmission, because CB2R KO mice could not be compared directly with C57BL/6J mice, which are only congenic controls for CB2R KO mice but not littermate controls.

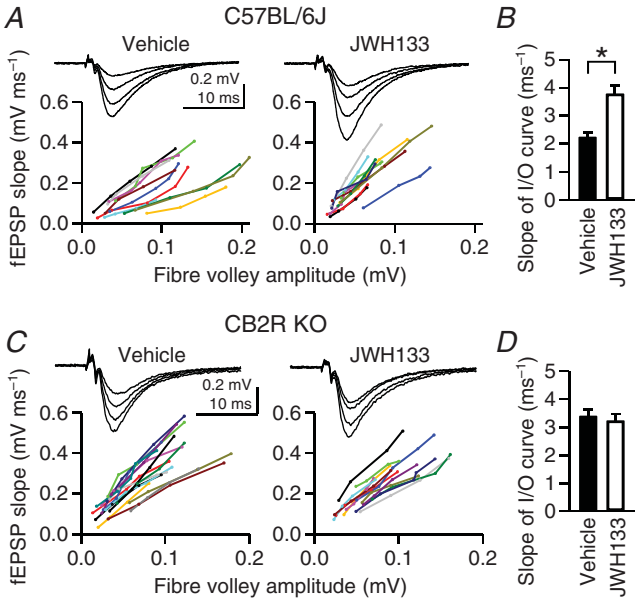

Figure 8. Chronic activation of CB2Rs in intact mice enhances excitatory synaptic transmission
A, field excitatory postsynaptic potentials (fEPSPs) were recorded from the CA1 stratum radiatum in acute hippocampal slices of C57BL/6J mice. Input–output (I/O) curves of fEPSPs were constructed from the rising slope of fEPSP against the amplitude of the presynaptic fibre volley. Mice were injected with JWH133 (5 mg kg^{-1}, I.P.) or vehicle once per day for 7–9 days. Acute hippocampal slices were made 24 h after the last injection. Each line represents one slice. *B*, the mean slope of the I/O curves was obtained from linear regression of individual I/O curves shown in *A*. *P = 0.0008, Student's unpaired t test. *C* and *D*, experiments were done as in *A* and *B*, but acute hippocampal slices were made from CB2R KO mice injected with JWH133 (5 mg kg^{-1}, I.P.) or vehicle once per day for 7–9 days.

Discussion

The present study shows that chronic activation of CB2Rs in the hippocampus increases mEPSC frequency and spine density via ERK-dependent signalling pathways. These effects of CB2Rs on synapses are specific for glutamatergic synapses after chronic, but not acute, activation of CB2Rs (e.g. for 7–10 days) and do not involve changes in presynaptic properties such as P_r or RRP size.

Chronic treatment of rodents *in vivo* with Δ^9-THC reduces the expression of ionotropic glutamate receptors (e.g. GluA1, GluN2A and GluN2B) and the magnitude of long-term potentiation (LTP) of glutamatergic transmission by specifically activating CB1Rs (Hoffman *et al.* 2007; Fan *et al.* 2010). In addition to the downregulation of excitatory synapses, long-term exposure to Δ^9-THC increases the I/O relationship of fEPSP and/or glutamatergic P_r (Hoffman *et al.* 2007; Fan *et al.* 2010). It has not been determined whether CB1Rs also mediate the Δ^9-THC-induced increases in excitatory synaptic transmission. Given that Δ^9-THC is a co-agonist for CB1Rs and CB2Rs, it is possible that some of the effects of chronic exposure to Δ^9-THC may be mediated by CB2Rs. Our data suggest that in particular, upregulation of glutamatergic synapses by chronic treatment with Δ^9-THC needs to be examined carefully in relationship to CB2R because chronic activation of CB2Rs can increase mEPSC frequency (Figs 1 and 2), spine density (Fig. 4) and the I/O relationship of fEPSP (Fig. 8). When rodents are repeatedly injected with a CB1R/CB2R co-agonist, e.g. Δ^9-THC or WIN55212-2, the synaptic density of CA1 pyramidal cells may be increased (Tagliaferro *et al.* 2006) or decreased (Chen *et al.* 2013), but it is unclear which type of cannabinoid receptor is involved in such effects. Once the role of CB1Rs in regulating synaptic density is determined, our results of the CB2R-mediated increase in spine density may help to reconcile these contradictory observations.

Both 2-AG and anandamide can activate CB2Rs, though 2-AG is a full agonist and anandamide is a partial agonist (Mechoulam *et al.* 1995; Showalter *et al.* 1996; Sugiura *et al.* 2000). 2-Arachidonoylglycerol and anandamide have 3- to 4-fold higher affinity for the CB1R than for the CB2R (Mechoulam *et al.* 1995; Showalter *et al.* 1996), and Δ^9-THC binds to the CB1R and the CB2R with the same affinity (Showalter *et al.* 1996). Therefore, it is conceivable that both receptors in the brain may be activated if the levels of endocannabinoids are chronically elevated in pathological situations (Di Marzo & Petrosino, 2007) or with long-term intake of marijuana. Endocannabinoids are indeed implicated to induce CB2R-dependent signalling cascades. For example, CB2R KO (Racz *et al.* 2008; Ortega-Alvaro *et al.* 2011; García-Gutiérrez *et al.* 2013), knock-down (Onaivi *et al.* 2008) or overexpression

(Aracil-Fernández *et al.* 2012; Romero-Zerbo *et al.* 2012) in mice induces neuropsychiatric phenotypes, and blocking endocannabinoid degradation reduces anxiety via CB2R (Busquets-Garcia *et al.* 2011). Further investigation is necessary to determine the physiological and pathological conditions in which endocannabinoids stimulate CB2Rs to modulate synaptic and neuronal functions.

In contrast to CB1Rs, CB2Rs exert their effects only after long-term stimulation, as shown by our data. In agreement with our observation, while acute activation of CB2Rs has little effect in intact mice, chronic administration of a CB2R agonist increases anxiety-like behaviour and reduces the expression of $GABA_A$ receptors (García-Gutiérrez *et al.* 2012). It is yet unclear why prolonged stimulation is required for CB2Rs to exert their effects. In principle, CB2R-induced phosphorylation of ERK is not slow, because activation of CB2Rs in HEK 293 cells and neuronal cell lines can phosphorylate ERK in minutes (Franklin & Carrasco, 2013; Zheng *et al.* 2013). The ERK-mediated changes in spine morphology can also occur rapidly, e.g. within hours during LTP (Segal, 2005; Bosch & Hayashi, 2012) or 24 h after treatment with brain-derived neurotrophic factor (Alonso *et al.* 2004). The amount of CB2R mRNA in the brain is only $<1\%$ of that of CB1R mRNA (Onaivi *et al.* 2006). It would be interesting to test whether such a low level of CB2R expression necessitates prolonged activation of CB2Rs for the accumulation of downstream signalling effectors. Although ERK-mediated increases in glutamatergic transmission and/or spine density are common consequences of LTP (Segal, 2005; Bosch & Hayashi, 2012), brain-derived neurotrophic factor treatment (Alonso *et al.* 2004) and chronic stimulation of CB2Rs, it is possible that the signalling cascade of CB2R–ERK–spine density might be distinct from the ERK signalling pathways for LTP and brain-derived neurotrophic factor treatment. For example, both homeostatic plasticity and LTP are expressed in the form of increases in AMPA receptors, but these two forms of plasticity have sharp contrasts in the time course and signalling molecules (Thiagarajan *et al.* 2007). The signalling cascades from CB2R to spines need to be determined in future studies.

Both ERK1 and ERK2 are involved in synaptic plasticity and memory (Thiels & Klann, 2001; Sweatt, 2004; Giovannini, 2006). ERK2 is critical for normal development, because ERK2 KO in mice is embryonically lethal (Aouadi *et al.* 2006). However, when ERK2 is knocked out in the CNS only, mice can survive, and the number of neurons and spine density are normal in the brain (Satoh *et al.* 2011). Reduced expression of ERK2 also has little effect on mouse survival and spine density in the hippocampus (Satoh *et al.* 2007). ERK1 KO mice display normal phenotypes in many aspects of synaptic transmission, e.g. I/O relationship of fEPSP, paired-pulse ratio of fEPSP and LTP of excitatory synapses (Selcher *et al.* 2001; Mazzucchelli *et al.* 2002). Therefore, the functions of glutamatergic synapses appear to be preserved by downregulation of ERK1 or ERK2 in the brain in spite of the importance of the kinases in synaptic plasticity. In accord with these reports, a reduction in the basal phosphorylation of ERK1/2 by treatment with PD0325901 alone (Fig. 7*C*) did not significantly downregulate mEPSC or spine density (Fig. 7*A* and *B*). If a decrease in ERK activity does not reduce spine density, as our data suggest (Fig. 7), the mechanism of reduced spine density in CB2R KO mice (García-Gutiérrez *et al.* 2013) might not simply be the reversed signalling of the CB2R-mediated increase in spine density. Mechanistic comparisons between CB2R-mediated increase and decrease in spine density will be another topic for intensive investigation.

Long-term stimulation of CB2Rs increased the density of thin spines selectively (Fig. 4*B*). Mushroom spines can transform to thin spines, e.g. during long-term depression of glutamatergic transmission (Nägerl *et al.* 2004; Zhou *et al.* 2004), but this transformation seemed unlikely to have occurred after chronic treatment with a CB2R agonist, because CB2R activation did not reduce the density of mushroom spines (Fig. 4*B*). The increase in the density of total spines suggests that thin spines might be generated anew, because the formation, elimination and structural changes of thin spines are more dynamic compared with those of mushroom spines (Bourne & Harris, 2007). Filopodia are formed *de novo* during development or LTP, and often lack presynaptic partners (Bourne & Harris, 2007; Bosch & Hayashi, 2012). The thin spines in our data can be distinguished from filopodia because the upper limit of spine length in our analysis ($3\ \mu$m) must have excluded most filopodia, which are often $>3\ \mu$m (Maletic-Savatic *et al.* 1999). Activation of CB2Rs increased spine density by $\sim$20% (Fig. 4*A*), whereas it increased mEPSC frequency by $\sim$50% (Fig. 1*C* and *D*). It is possible that factors other than spine density might have contributed to the increase in mEPSC frequency. For instance, an increase in the total dendritic length of a neuron would also make mEPSCs more frequent.

Although chronic blockade of CB2Rs with SR144528 for 7–10 days had no effect on mEPSC frequency in slice cultures (Fig. 1*F*), electron micrographs show that the KO of CB2Rs in mice reduces hippocampal spine density (García-Gutiérrez *et al.* 2013). This discrepancy could be because CB2Rs are non-functional in CB2R KO mice for a longer period of time from birth. It should be tested whether spine density is also reduced by treatment of wild-type tissue with a CB2R antagonist for a more extended period of time with an early onset. Our data show that inhibitory synaptic transmission was not affected by acute or chronic activation of CB2Rs, but in other studies acute stimulation of CB2Rs has reduced the amplitude of spontaneous IPSCs (but not mIPSCs) in the entorhinal

cortex (Morgan *et al.* 2009) and inhibited K^+-evoked GABA release from synaptosomes (Ando *et al.* 2012). Chronic activation of CB2Rs increases the expression of $GABA_A$ receptors (García-Gutiérrez *et al.* 2012). The reason for this discrepancy is unclear, but the differences in experimental conditions might be a possibility. For example, spontaneous IPSCs (Morgan *et al.* 2009) were recorded with excitatory and inhibitory networks intact, i.e. with only postsynaptic glutamate receptors blocked, and therefore, any changes in the excitability or P_r of a subset of neurons might alter the network activity, resulting in changes in spontaneous IPSCs. The *in vivo* route of drug administration (García-Gutiérrez *et al.* 2012), brain areas (Morgan *et al.* 2009; García-Gutiérrez *et al.* 2012) and the intactness of neurons (Ando *et al.* 2012) could also have contributed to the differences in the results.

In the hippocampus, CB2Rs are present in microglia (Sviženská *et al.* 2008; Atwood & Mackie, 2010), pyramidal neurons and interneurons (Gong *et al.* 2006; Onaivi *et al.* 2006; Brusco *et al.* 2008). It is critical to locate the CB2Rs that mediate the increases in mEPSC frequency and spine density to understand the mechanisms of CB2R action, e.g. cell-autonomous and network-effect mechanisms. If CB2Rs increase spine density in a cell-autonomous manner, the activation of CB2Rs in pyramidal cells may exert its effect only within the cell where those CB2Rs are present. Then, effector molecules downstream of CB2R can be intracellular messengers. A non-cell-autonomous or network-effect scenario is also possible; activation of CB2Rs in other pyramidal cells, interneurons and/or microglia might cause changes in network activity and hence increases in spine density more broadly. Intercellular signalling molecules may play a role in this case. To determine the mechanisms, it will be essential to stimulate CB2Rs only in a specific type of cell, as by knocking out or expressing CB2Rs in a certain type of cell.

The CB2R KO mice show impaired aversive memory consolidation (García-Gutiérrez *et al.* 2013), increased neuropathic pain (Racz *et al.* 2008) and schizophrenia-like behaviours (Ortega-Alvaro *et al.* 2011). Overexpression of CB2R in mice decreases the motor response to cocaine (Aracil-Fernández *et al.* 2012) and reduces food consumption (Romero-Zerbo *et al.* 2012). In humans, the polymorphism of *CNR2*, which encodes CB2R, is related to schizophrenia (Ishiguro *et al.* 2010; Tong *et al.* 2013), depression (Onaivi *et al.* 2008) and bipolar disorder (Minocci *et al.* 2011). A decrease in spine density is one of the hallmarks of individuals with schizophrenia (Jones *et al.* 2011), anxiety and depression (Wang *et al.* 2013), and CB2Rs are implicated in all of these disorders. It will be interesting to determine whether CB2Rs are involved in the spine pathology of such disorders and whether CB2R agonists can be used as a therapeutic tool for pathological spine loss.

References

Alger BE (2002). Retrograde signaling in the regulation of synaptic transmission: focus on endocannabinoids. *Prog Neurobiol* **68**, 247–286.

Alonso M, Medina JH & Pozzo-Miller L (2004). ERK1/2 activation is necessary for BDNF to increase dendritic spine density in hippocampal CA1 pyramidal neurons. *Learn Mem* **11**, 172–178.

Anand P, Whiteside G, Fowler CJ & Hohmann AG (2009). Targeting CB_2 receptors and the endocannabinoid system for the treatment of pain. *Brain Res Rev* **60**, 255–266.

Ando RD, Biro J, Csolle C, Ledent C & Sperlagh B (2012). The inhibitory action of exo- and endocannabinoids on [^{3}H]GABA release are mediated by both CB_1 and CB_2 receptors in the mouse hippocampus. *Neurochem Int* **60**, 145–152.

Aouadi M, Binetruy B, Caron L, Le Marchand-Brustel Y & Bost F (2006). Role of MAPKs in development and differentiation: lessons from knockout mice. *Biochimie* **88**, 1091–1098.

Aracil-Fernández A, Trigo JM, García-Gutiérrez MS, Ortega-Álvaro A, Ternianov A, Navarro D, Robledo P, Berbel P, Maldonado R & Manzanares J (2012). Decreased cocaine motor sensitization and self-administration in mice overexpressing cannabinoid CB_2 receptors. *Neuropsychopharmacology* **37**, 1749–1763.

Atwood BK & Mackie K (2010). CB_2: a cannabinoid receptor with an identity crisis. *Br J Pharmacol* **160**, 467–479.

Bosch M & Hayashi Y (2012). Structural plasticity of dendritic spines. *Curr Opin Neurobiol* **22**, 383–388.

Bourne J & Harris KM (2007). Do thin spines learn to be mushroom spines that remember? *Curr Opin Neurobiol* **17**, 381–386.

Brusco A, Tagliaferro P, Saez T & Onaivi ES (2008). Postsynaptic localization of CB2 cannabinoid receptors in the rat hippocampus. *Synapse* **62**, 944–949.

Burrone J, O'Byrne M & Murthy VN (2002). Multiple forms of synaptic plasticity triggered by selective suppression of activity in individual neurons. *Nature* **420**, 414–418.

Busquets-Garcia A, Puighermanal E, Pastor A, de la Torre R, Maldonado R & Ozaita A (2011). Differential role of anandamide and 2-arachidonoylglycerol in memory and anxiety-like responses. *Biol Psychiatry* **70**, 479–486.

Castillo PE, Younts TJ, Chávez AE & Hashimotodani Y (2012). Endocannabinoid signaling and synaptic function. *Neuron* **76**, 70–81.

Chen R, Zhang J, Fan N, Teng ZQ, Wu Y, Yang H, Tang YP, Sun H, Song Y & Chen C (2013). Δ^9-THC-caused synaptic and memory impairments are mediated through COX-2 signaling. *Cell* **155**, 1154–1165.

Chevaleyre V, Takahashi KA & Castillo PE (2006). Endocannabinoid-mediated synaptic plasticity in the CNS. *Annu Rev Neurosci* **29**, 37–76.

Demuth DG & Molleman A (2006). Cannabinoid signalling. *Life Sci* **78**, 549–563.

den Boon FS, Chameau P, Schaafsma-Zhao Q, van Aken W, Bari M, Oddi S, Kruse CG, Maccarrone M, Wadman WJ & Werkman TR (2012). Excitability of prefrontal cortical pyramidal neurons is modulated by activation of intracellular type-2 cannabinoid receptors. *Proc Natl Acad Sci USA* **109**, 3534–3539.

Devane WA, Dysarz FA 3rd, Johnson MR, Melvin LS & Howlett AC (1988). Determination and characterization of a cannabinoid receptor in rat brain. *Mol Pharmacol* **34**, 605–613.

Di Marzo V & Petrosino S (2007). Endocannabinoids and the regulation of their levels in health and disease. *Curr Opin Lipidol* **18**, 129–140.

Fan N, Yang H, Zhang J & Chen C (2010). Reduced expression of glutamate receptors and phosphorylation of CREB are responsible for *in vivo* Δ9-THC exposure-impaired hippocampal synaptic plasticity. *J Neurochem* **112**, 691–702.

Fernández-Ruiz J, Romero J, Velasco G, Tolón RM, Ramos JA & Guzmán M (2007). Cannabinoid CB_2 receptor: a new target for controlling neural cell survival? *Trends Pharmacol Sci* **28**, 39–45.

Franklin JM & Carrasco GA (2013). Cannabinoid receptor agonists upregulate and enhance serotonin 2A ($5\text{-}HT_{2A}$) receptor activity via ERK1/2 signaling. *Synapse* **67**, 145–159.

García-Gutiérrez MS, García-Bueno B, Zoppi S, Leza JC & Manzanares J (2012). Chronic blockade of cannabinoid CB_2 receptors induces anxiolytic-like actions associated with alterations in $GABA_A$ receptors. *Br J Pharmacol* **165**, 951–964.

García-Gutiérrez MS, Ortega-Álvaro A, Busquets-García A, Pérez-Ortiz JM, Caltana L, Ricatti MJ, Brusco A, Maldonado R & Manzanares J (2013). Synaptic plasticity alterations associated with memory impairment induced by deletion of CB2 cannabinoid receptors. *Neuropharmacology* **73**, 388–396.

Giovannini MG (2006). The role of the extracellular signal-regulated kinase pathway in memory encoding. *Rev Neurosci* **17**, 619–634.

Gong JP, Onaivi ES, Ishiguro H, Liu QR, Tagliaferro PA, Brusco A & Uhl GR (2006). Cannabinoid CB2 receptors: immunohistochemical localization in rat brain. *Brain Res* **1071**, 10–23.

Han S, Thatte J, Buzard DJ & Jones RM (2013). Therapeutic utility of cannabinoid receptor type 2 (CB_2) selective agonists. *J Med Chem* **56**, 8224–8256.

Hoffman AF, Oz M, Yang R, Lichtman AH & Lupica CR (2007). Opposing actions of chronic Δ^9-tetrahydrocannabinol and cannabinoid antagonists on hippocampal long-term potentiation. *Learn Mem* **14**, 63–74.

Ishiguro H, Horiuchi Y, Ishikawa M, Koga M, Imai K, Suzuki Y, Morikawa M, Inada T, Watanabe Y, Takahashi M, Someya T, Ujike H, Iwata N, Ozaki N, Onaivi ES, Kunugi H, Sasaki T, Itokawa M, Arai M, Niizato K, Iritani S, Naka I, Ohashi J, Kakita A, Takahashi H, Nawa H & Arinami T (2010). Brain cannabinoid CB2 receptor in schizophrenia. *Biol Psychiatry* **67**, 974–982.

Jhaveri MD, Sagar DR, Elmes SJ, Kendall DA & Chapman V (2007). Cannabinoid CB_2 receptor-mediated anti-nociception in models of acute and chronic pain. *Mol Neurobiol* **36**, 26–35.

Jones CA, Watson DJ & Fone KC (2011). Animal models of schizophrenia. *Br J Pharmacol* **164**, 1162–1194.

Kano M, Ohno-Shosaku T, Hashimotodani Y, Uchigashima M & Watanabe M (2009). Endocannabinoid-mediated control of synaptic transmission. *Physiol Rev* **89**, 309–380.

Katona I & Freund TF (2012). Multiple functions of endocannabinoid signaling in the brain. *Annu Rev Neurosci* **35**, 529–558.

Katona I, Sperlágh B, Sík A, Käfalvi A, Vizi ES, Mackie K & Freund TF (1999). Presynaptically located CB1 cannabinoid receptors regulate GABA release from axon terminals of specific hippocampal interneurons. *J Neurosci* **19**, 4544–4558.

Maletic-Savatic M, Malinow R & Svoboda K (1999). Rapid dendritic morphogenesis in CA1 hippocampal dendrites induced by synaptic activity. *Science* **283**, 1923–1927.

Marsicano G & Lutz B (1999). Expression of the cannabinoid receptor CB1 in distinct neuronal subpopulations in the adult mouse forebrain. *Eur J Neurosci* **11**, 4213–4225.

Matsuda LA, Lolait SJ, Brownstein MJ, Young AC & Bonner TI (1990). Structure of a cannabinoid receptor and functional expression of the cloned cDNA. *Nature* **346**, 561–564.

Mazzucchelli C, Vantaggiato C, Ciamei A, Fasano S, Pakhotin P, Krezel W, Welzl H, Wolfer DP, Pagès G, Valverde O, Marowsky A, Porrazzo A, Orban PC, Maldonado R, Ehrengruber MU, Cestari V, Lipp HP, Chapman PF, Pouysségur J & Brambilla R (2002). Knockout of ERK1 MAP kinase enhances synaptic plasticity in the striatum and facilitates striatal-mediated learning and memory. *Neuron* **34**, 807–820.

Mechoulam R, Ben-Shabat S, Hanus L, Ligumsky M, Kaminski NE, Schatz AR, Gopher A, Almog S, Martin BR, Compton DR, Pertwee RG, Griffin G, Bayewitch M, Barg J & Vogel Z (1995). Identification of an endogenous 2-monoglyceride, present in canine gut, that binds to cannabinoid receptors. *Biochem Pharmacol* **50**, 83–90.

Minocci D, Massei J, Martino A, Milianti M, Piz L, Di Bello D, Sbrana A, Martinotti E, Rossi AM & Nieri P (2011). Genetic association between bipolar disorder and 524A>C (Leu133Ile) polymorphism of *CNR2* gene, encoding for CB2 cannabinoid receptor. *J Affect Disord* **134**, 427–430.

Morgan NH, Stanford IM & Woodhall GL (2009). Functional CB2 type cannabinoid receptors at CNS synapses. *Neuropharmacology* **57**, 356–368.

Munro S, Thomas KL & Abu-Shaar M (1993). Molecular characterization of a peripheral receptor for cannabinoids. *Nature* **365**, 61–65.

Nägerl UV, Eberhorn N, Cambridge SB & Bonhoeffer T (2004). Bidirectional activity-dependent morphological plasticity in hippocampal neurons. *Neuron* **44**, 759–767.

Navarrete F, Pérez-Ortiz JM & Manzanares J (2012). Cannabinoid CB_2 receptor-mediated regulation of impulsive-like behaviour in DBA/2 mice. *Br J Pharmacol* **165**, 260–273.

Onaivi ES, Ishiguro H, Gong JP, Patel S, Meozzi PA, Myers L, Perchuk A, Mora Z, Tagliaferro PA, Gardner E, Brusco A, Akinshola BE, Hope B, Lujilde J, Inada T, Iwasaki S, Macharia D, Teasenfitz L, Arinami T & Uhl GR (2008). Brain neuronal CB2 cannabinoid receptors in drug abuse and depression: from mice to human subjects. *PLoS One* **3**, e1640.

Onaivi ES, Ishiguro H, Gong JP, Patel S, Perchuk A, Meozzi PA, Myers L, Mora Z, Tagliaferro P, Gardner E, Brusco A, Akinshola BE, Liu QR, Hope B, Iwasaki S, Arinami T, Teasenfitz L & Uhl GR (2006). Discovery of the presence and functional expression of cannabinoid CB2 receptors in brain. *Ann NY Acad Sci* **1074**, 514–536.

Onaivi ES, Ishiguro H, Gu S & Liu QR (2012). CNS effects of CB2 cannabinoid receptors: beyond neuro-immuno-cannabinoid activity. *J Psychopharmacol* **26**, 92–103.

Ortega-Alvaro A, Aracil-Fernández A, García-Gutiérrez MS, Navarrete F & Manzanares J (2011). Deletion of CB_2 cannabinoid receptor induces schizophrenia-related behaviors in mice. *Neuropsychopharmacology* **36**, 1489–1504.

Racz I, Nadal X, Alferink J, Baños JE, Rehnelt J, Martín M, Pintado B, Gutierrez-Adan A, Sanguino E, Manzanares J, Zimmer A & Maldonado R (2008). Crucial role of CB_2 cannabinoid receptor in the regulation of central immune responses during neuropathic pain. *J Neurosci* **28**, 12125–12135.

Rodriguez A, Ehlenberger DB, Dickstein DL, Hof PR & Wearne SL (2008). Automated three-dimensional detection and shape classification of dendritic spines from fluorescence microscopy images. *PLoS One* **3**, e1997.

Romero-Zerbo SY, Garcia-Gutierrez MS, Suárez J, Rivera P, Ruz-Maldonado I, Vida M, Rodriguez de Fonseca F, Manzanares J & Bermúdez-Silva FJ (2012). Overexpression of cannabinoid CB2 receptor in the brain induces hyperglycaemia and a lean phenotype in adult mice. *J Neuroendocrinol* **24**, 1106–1119.

Rosenmund C & Stevens CF (1996). Definition of the readily releasable pool of vesicles at hippocampal synapses. *Neuron* **16**, 1197–1207.

Satoh Y, Endo S, Ikeda T, Yamada K, Ito M, Kuroki M, Hiramoto T, Imamura O, Kobayashi Y, Watanabe Y, Itohara S & Takishima K (2007). Extracellular signal-regulated kinase 2 (ERK2) knockdown mice show deficits in long-term memory; ERK2 has a specific function in learning and memory. *J Neurosci* **27**, 10765–10776.

Satoh Y, Endo S, Nakata T, Kobayashi Y, Yamada K, Ikeda T, Takeuchi A, Hiramoto T, Watanabe Y & Kazama T (2011). ERK2 contributes to the control of social behaviors in mice. *J Neurosci* **31**, 11953–11967.

Schneggenburger R, Meyer AC & Neher E (1999). Released fraction and total size of a pool of immediately available transmitter quanta at a calyx synapse. *Neuron* **23**, 399–409.

Segal M (2005). Dendritic spines and long-term plasticity. *Nat Rev Neurosci* **6**, 277–284.

Selcher JC, Nekrasova T, Paylor R, Landreth GE & Sweatt JD (2001). Mice lacking the ERK1 isoform of MAP kinase are unimpaired in emotional learning. *Learn Mem* **8**, 11–19.

Showalter VM, Compton DR, Martin BR & Abood ME (1996). Evaluation of binding in a transfected cell line expressing a peripheral cannabinoid receptor (CB2): identification of cannabinoid receptor subtype selective ligands. *J Pharmacol Exp Ther* **278**, 989–999.

Stevens CF & Williams JH (2007). Discharge of the readily releasable pool with action potentials at hippocampal synapses. *J Neurophysiol* **98**, 3221–3229.

Sugiura T, Kondo S, Kishimoto S, Miyashita T, Nakane S, Kodaka T, Suhara Y, Takayama H & Waku K (2000). Evidence that 2-arachidonoylglycerol but not *N*-palmitoylethanolamine or anandamide is the physiological ligand for the cannabinoid CB2 receptor. Comparison of the agonistic activities of various cannabinoid receptor ligands in HL-60 cells. *J Biol Chem* **275**, 605–612.

Sviženská I, Dubový P & Šulcová A (2008). Cannabinoid receptors 1 and 2 (CB1 and CB2), their distribution, ligands and functional involvement in nervous system structures — a short review. *Pharmacol Biochem Behav* **90**, 501–511.

Sweatt JD (2004). Mitogen-activated protein kinases in synaptic plasticity and memory. *Curr Opin Neurobiol* **14**, 311–317.

Tagliaferro P, Javier Ramos A, Onaivi ES, Evrard SG, Lujilde J & Brusco A (2006). Neuronal cytoskeleton and synaptic densities are altered after a chronic treatment with the cannabinoid receptor agonist WIN 55,212-2. *Brain Res* **1085**, 163–176.

Thiagarajan TC, Lindskog M, Malgaroli A & Tsien RW (2007). LTP and adaptation to inactivity: overlapping mechanisms and implications for metaplasticity. *Neuropharmacology* **52**, 156–175.

Thiels E & Klann E (2001). Extracellular signal-regulated kinase, synaptic plasticity, and memory. *Rev Neurosci* **12**, 327–345.

Tong D, He S, Wang L, Jin L, Si P & Cheng X (2013). Association of single-nucleotide polymorphisms in the cannabinoid receptor 2 gene with schizophrenia in the Han Chinese population. *J Mol Neurosci* **51**, 454–460.

Van Sickle MD, Duncan M, Kingsley PJ, Mouihate A, Urbani P, Mackie K, Stella N, Makriyannis A, Piomelli D, Davison JS, Marnett LJ, Di Marzo V, Pittman QJ, Patel KD & Sharkey KA (2005). Identification and functional characterization of brainstem cannabinoid CB_2 receptors. *Science* **310**, 329–332.

Wang G, Cheng Y, Gong M, Liang B, Zhang M, Chen Y, Zhang C, Yuan X & Xu J (2013). Systematic correlation between spine plasticity and the anxiety/depression-like phenotype induced by corticosterone in mice. *Neuroreport* **24**, 682–687.

Wilson RI, Kunos G & Nicoll RA (2001). Presynaptic specificity of endocannabinoid signaling in the hippocampus. *Neuron* **31**, 453–462.

Zheng C, Chen L, Chen X, He X, Yang J, Shi Y & Zhou N (2013). The second intracellular loop of the human cannabinoid CB2 receptor governs G protein coupling in coordination with the carboxyl terminal domain. *PLoS One* **8**, e63262.

Zhou Q, Homma KJ & Poo MM (2004). Shrinkage of dendritic spines associated with long-term depression of hippocampal synapses. *Neuron* **44**, 749–757.

Additional information

Competing interests

None declared.

Author contributions

J.K. and Y.L. conceived and designed the research, performed experiments, collected, analysed and interpreted data, prepared figures, wrote the manuscript and approved the final version to be published.

Funding

This work was supported by the National Institute on Aging Grant R01AG036794.

Acknowledgements

The authors thank Drs Bo-Shiun Chen, Bradley Alger, Thomas Abrams, Scott Thompson and Jianhua Xu and members of the Kim laboratory for advice and/or technical support.